Nucleophilic Attack at Selenium in Diselenides and Selenosulfides. A Computational Study

Steven M. Bachrach,* Dustin W. Demoin, Michelle Luk, and James V. Miller Jr.

Department of Chemistry, Trinity University, 1 Trinity Place, San Antonio, Texas 78212

Received: December 22, 2003; In Final Form: February 27, 2004

Nucelophilic substitution at selenium is examined using the B3LYP and MP2 methods. Various nucleophiles (HS^-, CH_3S^-, HSe^-, and CH_3Se^-) and substrates (R_1SSeR_2 and R_1SeSeR_2 with R_1 and R_2 = H or Me) are used to model substitution at selenium in diselenides and selenosulfides. In all cases, the mechanism is addition−elimination. A stable hypercoordinate selenium intermediate lies in a well that is 8−14 kcal mol^{-1} deep. Nucleophilic attack at selenium is both kinetically and thermodynamically more favorable than at sulfur.

Introduction

Proteins containing selenium play a variety of important roles in cellular activity.[1,2] Glutathione peroxidase reduces peroxides.[3] Thioredoxin reductase is used to regenerate thioredoxin and other antioxidants.[4,5] While the functions of selenoprotein P are not certain, it has been suggested to supply selenium to various organs[6,7] and chelate heavy metals.[1] These three selenoproteins are also capable of protecting against peroxynitrite, formed by the reaction of NO with superoxide.[8] Iodothyronine deiodinase is involved in thyroid hormone regulation.[9] All of these selenium-containing proteins possess a selenosulfide linkage that has often been implicated in their activity; the Se−S bond is cleaved typically through redox chemistry or nucleophilic attack at either the sulfur or selenium end.[10−13]

A small number of studies pertaining to the mechanism of nucleophilic attack on the selenosulfide bond have appeared. The first, and most detailed, is the study by Kice and Slebocka-Tilk[14] on the reaction RSSeSR + RSH, with R = *n*-Bu, *i*-Pr, or *t*-Bu. Their kinetics study was performed in 60% dioxane, with a RS^-−RSH buffer, and monitored using stopped-flow spectrophotometry. They found a number of important results: (1) the nucleophile is thiolate not thiol, (2) attack on selenium is faster than at sulfur, and (3) for attack at selenium where R = *tert*-butyl, E_a = 18.6 kcal mol^{-1}, and $\Delta S^{\ddagger} = -0.7$ eu, but for attack at sulfur, E_a = 8.6 kcal mol^{-1} and $\Delta S^{\ddagger} = -23$ eu. The reaction of phenyllithium with the same bis(alkylthio)selenides indicated that attack is about 60 times faster at selenium than at sulfur when the alkyl group is *tert*-butyl, the rates are about identical when *i*-propyl is used, and no attack at selenium was observed when the alkyl group is *n*-butyl. They concluded that attack at sulfur occurs by the S_N2 pathway. However, because of the very small and slightly negative $\Delta S^{\ddagger}$, they suggest that nucleophilic substitution at selenium either occurs via either (a) an S_N2 pathway but with a much less negative entropy of activation than typically observed, or (b) a single-electron-transfer mechanism where the slow step is the transfer of the electron from thiolate to the selenide. Rabenstein and co-workers[15] investigated the reaction of D-penicillamine with bis-(D-penicillamine)selenide in aqueous solution, monitoring the kinetics by NMR line broadening. They found that attack at selenium is much faster than at sulfur, consistent with Kice's result for a bulky group on sulfur. However, they also found that the reaction at selenium is much faster than the reaction of *t*-BuS^- with *t*-BuSSeSBu-*t*.

While the thiolate−disulfide exchange has been extensively examined,[16] only one study has appeared on the kinetics of the selenolate-diselenide exchange. Rabenstein et al.,[17] again using NMR line broadening techniques, looked at the kinetics for the exchange R*SeH + RSeSeR → R*SeSeR + RSeH where R is $H_3NCH_2CH_2$. The nucleophile was found to be the selenolate, not the selenol. In comparison to the thiolate−disulfide exchange with the same R group, the selenium case is about 10^7 times faster at physiological pH. They presumed the mechanism is S_N2 on the basis of the analogy to the thiolate−disulfide exchange. They rationalized the faster selenium reaction based on selenium being more polarizable than sulfur, making it a better nucleophile and a better leaving group. Further, the Se−Se bond is weaker than the S−S bond by nearly 20 kcal mol^{-1}. There are a few examples of exploiting the cleavage of the Se−Se bond to create selenolate ions for synthetic purposes.[18]

We have extensively examined nucleophilic substitution at sulfur, including the thiolate-disulfide exchange in a variety of systems (cyclic and acyclic) and phases (gas and aqueous).[19−25] We have found a strong preference for the addition−elimination mechanism in the gas phase, and some evidence of this mechanism even in solution, though the S_N2 mechanism is also viable in solution. We have also demonstrated that electron-withdrawing substituents on sulfur will stabilize the hypercoordinate intermediate; for the reaction of chloride with SCl_2[26] or $SOCl_2$,[27] the hypercoordinate intermediate is readily identifiable in the gas phase. This concept has recently been extended to selenium − the gas-phase reaction of chloride and $SeCl_2$ produces stable $SeCl_3^-$.[28] DFT computations of this reaction (and also the reaction of chloride with $SeOCl_2$) indicate a potential energy surface devoid of all features except the stable, hypercoordinate intermediate; the reagents combine together without a barrier. This suggests an addition−elimination mechanism for nucleophilic substitution at selenium.

In this study we present computations of model gas-phase nucleophilic substitution reactions at selenium. Reactions 1−4 are identity reactions for substitution at selenium in diselenides. The reactivities of selenosulfides are examined in reactions 5−10 where we have examined nucleophilic attack at either selenium or sulfur. We chose to use thiolate nucleophiles for

Corresponding author. E-mail: sbachrach@trinity.edu.

10.1021/jp037972o CCC: $27.50
Published on Web 04/14/2004

these reactions since in biological systems the nucleophile is often glutathione. For all of these reactions at selenium, the mechanism for nucleophilic substitution is addition−elimination.

$R_1Se^- + R_2SeSeR_1 \rightarrow R_1SeSeR_2 + R_1Se^-$	Reaction 1: $R_1 = R_2 = H$
	Reaction 2: $R_1 = Me$; $R_2 = H$
	Reaction 3: $R_1 = H$; $R_2 = Me$
	Reaction 4: $R_1 = Me$; $R_2 = Me$
$R_1S^- + R_2SeSR_1 \rightarrow R_1SSeR_2 + R_1S^-$	Reaction 5: $R_1 = H$; $R_2 = H$
	Reaction 6: $R_1 = Me$; $R_2 = H$
	Reaction 7: $R_1 = H$; $R_2 = Me$
$R_1S^- + R_2SeSR_1 \rightarrow R_1SSR_1 + R_2Se^-$	Reaction 8: $R_1 = H$; $R_2 = H$
	Reaction 9: $R_1 = Me$; $R_2 = H$
	Reaction 10: $R_1 = H$; $R_2 = Me$

Computational Methods

In our earliest study of the thiolate-disulfide exchange reaction, we noted a strong dependence of the topology of the potential energy surface (and thereby the reaction mechanism) on the computational method. Using a Hartree−Fock wavefunction,[19,29] a classic gas-phase S_N2 mechanism,[30] expressed by a double-well potential energy surface (PES), is found (Scheme 1a). The two wells correspond to ion−dipole complexes, which are separated by a single transition state displaying backside attack of the nucleophile. However, when electron correlation is included (MP2, MP4, CCSD, or DFT), the PES has three wells, an entrance and exit ion−dipole complex and an intermediate with a hypercoordinate sulfur (Scheme 1b). We anticipate that correlated methods will be needed to examine the nucleophilic substitution reaction at selenium (reactions 1−7), though we did examine reactions 1−4 at the HF/6-31+G* level. All reactions were calculated at MP2 and B3LYP to ascertain the effect of their differing treatment of electron correlation.[31,32]

Since reactions 1−10 include anionic species, the basis set must include diffuse functions.[33] Polarization functions are needed to adequately describe the different formal oxidation states of sulfur. The aug-cc-pVDZ[34] basis set could be employed for reactions 1 and 5−10 at B3LYP and MP2, but proved to be too large for the other reactions. We have therefore used the 6-31+G* basis set for reactions 1−4, and compare the two basis sets for reaction 1.

All structures were fully optimized. Transition states were located by using the standard Berny algorithm starting with an initial structure that had one imaginary frequency. Analytical frequencies were obtained for all structures to determine the nature of each critical point and also to correct the energies for zero-point vibrational energy (ZPE). The ZPEs were used without correction. All computations were performed using GAUSSIAN-98[35] or GAUSSIAN-03.[36]

Results

General Form of the PES. There are two stereochemical pathways for the substitution reactions: one where the substituent on the nucleophile and the leaving groups are syn, and one where the two substituents are anti. We have noted little energetic or geometric differences between the syn and anti pathways for substitution at sulfur;[19,22] nevertheless, we examined and report both pathways for reactions 1−4. Since again there is little energetic differences between these stereoisomeric pathways, we chose to examine just the anti pathways for reactions 5−10.

All gas-phase reactions involving ions and neutrals will first form an ion−dipole (or ion-induced dipole) complex. We have not located these structures and have assumed their existence in both the entrance and exit channels. The main purpose of this study is to ascertain the reaction mechanism, with a secondary interest in the stability of any intermediate, if any. Since the ion dipole complexes will appear regardless of the mechanism, their structure and energies are not essential.

SCHEME 1

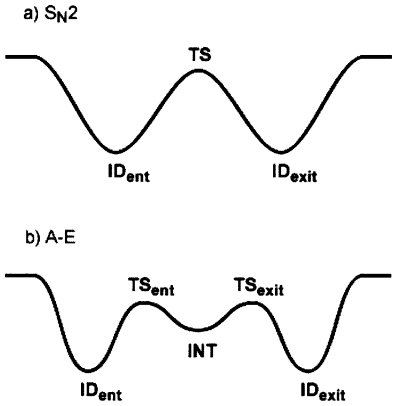

Our previous examination of substitution reactions at sulfur indicated that the HF method provides an inaccurate topology of the PES (Scheme 1).[19,22] The HF method predicts a surface with a single transition state (TS). This is rectified by inclusion of electron correlation; all methods that incorporate some treatment of electron correlation predict a triple-well PES (Scheme 1b) characterized by an entrance and exit channel ion−dipole complex connected to a stable intermediate through entrance and exit transitions states.

We anticipated that the HF method would fail to adequately describe the PES for nucleophilic substitution at selenium. We located the critical points for both the syn and anti pathways for reactions 1−4. For reactions 2−4 for both the syn and anti paths, we located a single TS only, corresponding to backside attack of the nucleophile. The PESs for these reactions look like Scheme 1a and are consistent with our HF results for substitution at sulfur. Interestingly, the PES for reaction 1 (both syn and anti) has three wells including a stable intermediate (Scheme 1b). However, recomputation of the surfaces for reactions 1−4 at either B3LYP or MP2 results in the triple-well potential only (Scheme 1b). Therefore, we will discuss only these correlated results hereafter.

Geometries. The optimized geometries of the transition states and intermediates for reactions 1−4 are drawn in Figure 1. Since these are identity reactions, the entrance and exit TSs are identical. All TSs are labeled as **Nx-TS**, where **N** designates the reaction number and **x** designates the relative stereochemistry: either **a** for anti or **s** for syn.

Reaction 1 involves small enough species that in addition to B3LYP/6-31+G* and MP2/6-31+G* computations, we could perform computations using the larger aug-cc-pVDZ basis set. There is very little difference between the geometries predicted with the two different basis sets; the covalently bonded Se−Se distances are slightly longer and the Se−Se−Se angle in the intermediates are slightly smaller using the larger basis set. These slight differences justify the use of the smaller 6-31+G* basis set for reactions 2−4. For reactions 5−10, which involve smaller molecules, we report the results using the larger aug-cc-pVDZ basis set.

A few trends are apparent in examining the structures of reaction 1; these hold for reactions 2−4 as well. First, the distances and angles in the TSs and intermediates for the syn and anti pathway are extremely similar, regardless of computational level employed. For example, the Se−Se distances in

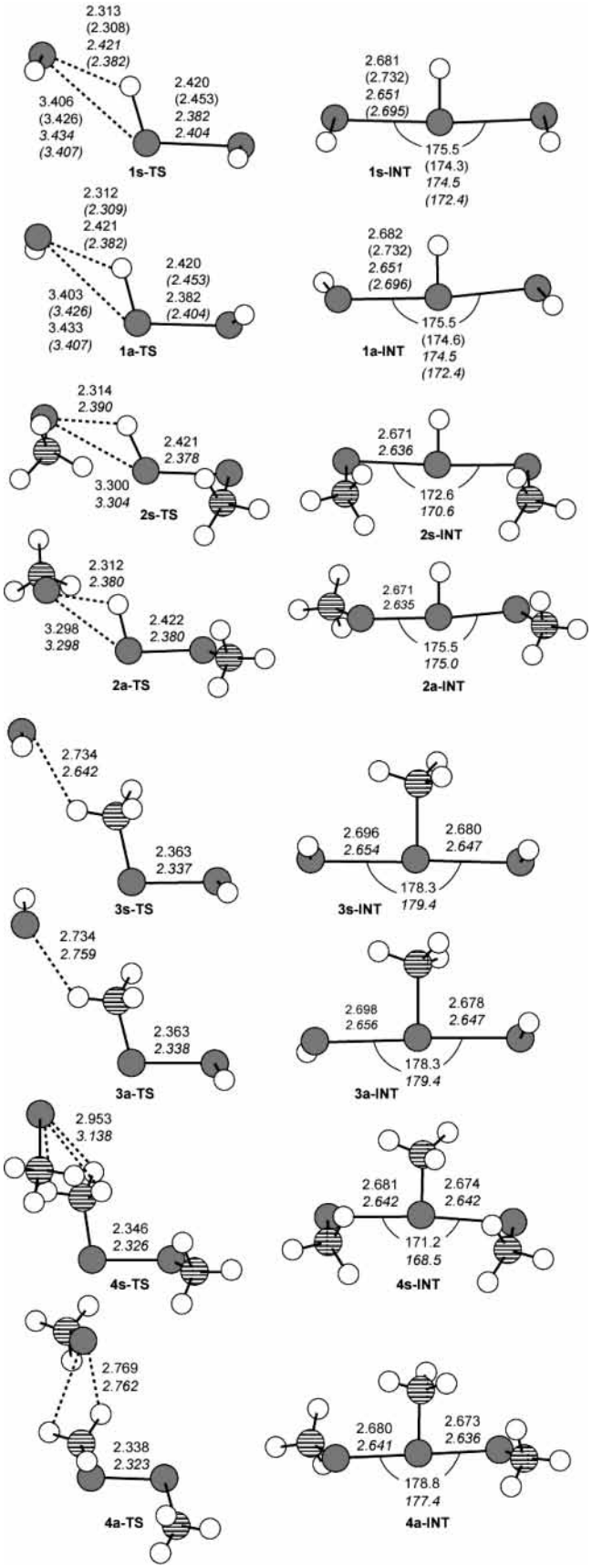

Figure 1. Optimized structures of the intermediates and transition states in reactions 1−4. All distances are in Å and all angles are in degrees. B3LYP/6-31+G* results are in plain text, B3LYP/aug-cc-pVDZ results are in parentheses, MP2/6-31+G* results are in italics, and MP2/aug-cc-pVDZ results are in parentheses and italics. Selenium atoms are indicated by the darkened circles, hydrogen atoms by the small open circles, and carbon atoms by the striped circles.

1s-INT and **1a-INT** differ by no more than 0.001 Å for any method. Second, MP2 predicts a slightly smaller Se−Se bond, with the difference no larger than 0.04 Å. In almost all of the intermediates, MP2 predicts a slightly smaller Se−Se−Se angle than does B3LYP. While we report both B3LYP and MP2 results for all reactions, there is general agreement as to the geometries of the critical points.

There are some interesting trends in terms of geometric changes along the reaction pathway. The Se−Se distance in the reactants of reaction 1−4 are listed in Table 1, with an average Se−Se distance of 2.33 Å. In the TSs for reactions 1 and 2, where the selenium under attack bears a hydrogen atom, the incoming nucleophile is weakly attracted to this hydrogen and begins to form a bond to selenium. This forming Se−Se bond distance is about 3.3 Å, while the other Se−Se bond lengthens by about 0.1 Å. In the TSs for reactions 3 and 4, the incoming nucleophile is associated only with the hydrogens of the methyl group and has not yet begun to form the new Se−Se bond. Consequently, the Se−Se bond has not stretched by very much. In the intermediates, the two Se−Se distances are either identical due to symmetry or nearly equidistant, differing by no more than 0.02 Å. The Se−Se distance ranges from 2.6 to 2.7 Å, about 0.3 Å longer than in the isolated diselenide.

Reactions 5−7 involve nucleophilic attack at selenium in a selenosulfide and can therefore be compared to reactions 1−4. Drawings of the optimized critical points (TSs and intermediates) for these reactions are shown in Figure 2. We have examined only the anti pathway since the geometries and energies (see below) of the syn and anti pathways for reactions 1−4 are so similar. As discussed above, the Se−S distance is shorter and the S−Se−S angle is smaller at MP2 than B3LYP, but these differences are very small (less than 0.05 Å and 2.2°). The forming S−Se distance is about 3.2 Å in **5-TS** and **6-TS**, and the other Se−S bond has lengthened by about 0.1 Å, similar to **1-TS** and **2-TS.** However, the forming S−Se distance is much longer in **7-TS** since here the nucleophile associates with a hydrogen on the methyl group. The other S−Se distance is little changed from reactant. The S−Se distances in the intermediates **5-INT**, **6-INT**, and **7-INT** are about 2.6 Å. The S−Se−S angles are all between 171.7° and 178.6°. These intermediates are structurally very similar to the intermediates in reactions 1−4.

The structures of the entrance TSs (labeled as **TSn**), intermediates and exit TSs (labled as **TSx**) for reactions 8−10 are drawn in Figure 3. These reactions involve nucleophilic substitution at sulfur with thiolate as the nucleophile and selenolate as the leaving group. These critical points are geometrically quite similar to TS and intermediates we have described for other substitution reactions at sulfur.[19,21,22] The only unusual structure is **9-INT**. We have typically observed S−S distances of about 2.5 to 2.9 Å in the intermediates; in **9-INT** this distance is very short (2.228 Å at B3LYP and 2.144 Å at MP2) and the S−Se distance is very long, over 3.1 Å. This intermediate is clearly much more product-like than any of the other intermediates.

Energies. The relative energies of the TSs and intermediates for reactions 1−7 (nucleophilic substitution at selenium) are listed in Table 2. A TS energy that is negative is not a misnomer. The TS connects the intermediate with the ion−dipole complex, not reactants. The ion−dipole complexes are always more stable than separated reactants. The TS does lie above both the ion−dipole complex and the intermediate, but below reactants. This is a typical PES for gas-phase substitution reactions.[30]

While the geometries of reaction 1 are relatively insensitive to both basis set and computational method, the energies show

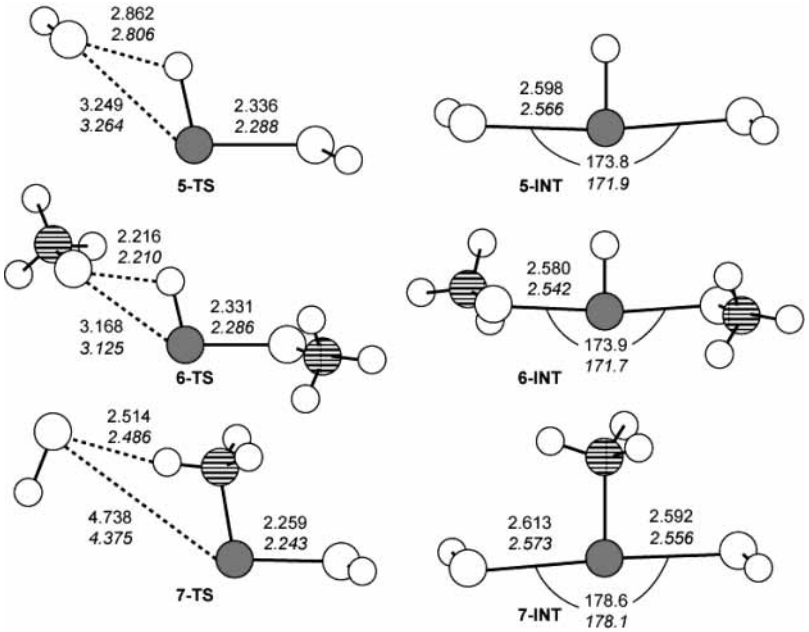

Figure 2. Optimized structures of the intermediates and transition states in reactions 5−7. B3LYP/aug-cc-pVDZ results are in plain text and MP2/aug-cc-pVDZ results are in italics. Sulfur atoms are indicated by large empty circles. See Figure 1 for all other details.

TABLE 1: Se−Se or Se−S Distance (Å) in the Reactants and Products

	B3LYP/ 6-31+G*	B3LYP/ aug-cc-pVDZ	MP2/ 6-31+G*	MP2/ aug-cc-pVDZ
HSeSeH	2.349	2.372	2.340	2.355
MeSeSeH	2.341		2.331	
MeSeSeMe	2.333		2.322	
HSeSH		2.244		2.231
HSeSMe		2.235		2.220
MeSeSH		2.238		2.225
HSSH		2.110		2.092
MeSSMe		2.102		2.084

more dependence. The relative energies of both the TS and intermediate are lower by about 4 kcal mol^{-1} using the smaller 6-31+G* basis set than with the aug-cc-pVDZ set. This is true for both the B3LYP and MP2 methods. Further, the B3LYP relative energies are about 1.5 kcal mol^{-1} lower (i.e., more negative) than the MP2 energies. However, the depth of the well the intermediate sits in, in other words the energy difference between the TS and the intermediate, is little affected by the basis set or method; it ranges from 8.22 to 9.37 kcal mol^{-1} for reaction 1. Therefore, any of the four methods provides essentially identical energies for the critical feature of the potential energy surface—the stability of the intermediate judged on the depth of its well.

The relative energies of the TSs and intermediates for the syn and anti paths of reaction 1 are nearly identical, differing by no more than 0.025 kcal mol^{-1} at any computational level. This is true for reactions 2−4 as well, justifying the decision to examine only the anti pathway for reactions 5−7.

The relative energies for reactions 1 and 2 are very similar, just as are the relative energies for reactions 3 and 4. The first pair models attack at selenium carrying a hydrogen atom while for the second pair the selenium under attack has a methyl group. The well depth for reactions 1 and 2 are about 8−9 kcal mol^{-1}. Reactions 5 and 6 also involve attack at selenium having a hydrogen atom, but the nucleophile and leaving groups are thiolates instead of selenolates. Nevertheless, the relative energies of the TSs and intermediates are similar to those of reactions 1 and 2: the well depths of all four reactions are within 1 kcal mol^{-1} of each other. On the other hand, the well depth is about 14 kcal mol^{-1} for reactions 3 and 4. Reaction 7 also has the attack at selenium with a methyl group, but its well depth is about 11 kcal mol^{-1}. For all seven reaction of nucleophilic substitution at selenium, the well depth of the intermediate is greater than that for analogous reactions at sulfur, where the intermediate well is no more that 5 kcal mol^{-1}.[22]

The energetics for nucleophilic attack by thiolate on the sulfur in selenosulfides (reactions 7−10) are listed in Table 3. Since the leaving group is a selenolate, these are not identity reactions. Reactions 8 and 9 are exothermic, while reaction 10 is endothermic. These reaction energies roughly reflect the relative basicities of the anions: CH_3S^- > HS^- > CH_3Se^- > HSe^- (see Table 4). In other words, reactions 8 and 9 are more favorable than reaction 10 because HSe^- is a better leaving group (weaker base) than CH_3Se^-.

As we have observed for many substitution reactions at sulfur,[19−23] the reaction surface for reactions 8−10 include a stable hypercoordinate intermediate. **8-INT** resides in a well with a depth of 4−5 kcal mol^{-1}, very typical for substitution at sulfur. The well for **10-INT** is asymmetric, due to the endothermicity of the reaction. The barrier from **10-INT** toward product is about 7 kcal mol^{-1}, while the barrier to reactant is only 2 kcal mol^{-1}. Again, we have observed well depths of this magnitude many times. **9-INT** sits in a very asymmetric well: the barrier toward reactant is about 11 kcal mol^{-1}, but the barrier forward is about 0.5 kcal mol^{-1}. The large barrier toward reactant is reminiscent of the deep wells seen in the reactions such as $Cl^- + SCl_2$,[26−28] where the transition state in fact disappears. The low barrier for exiting the intermediate reflects the very early nature of **9-TSx**; reaction 9 is the least endothermic of the three reactions in going from intermediate to product, consistent with the Hammond Postulate. Also, we have noted very small barriers for nucleophilic attack at sulfur bearing a methyl group,[19,20,22] which is the reverse of reaction 9.

Discussion

Our main interest here is to determine the mechanism of nucleophilic substitution at selenium. The potential energy

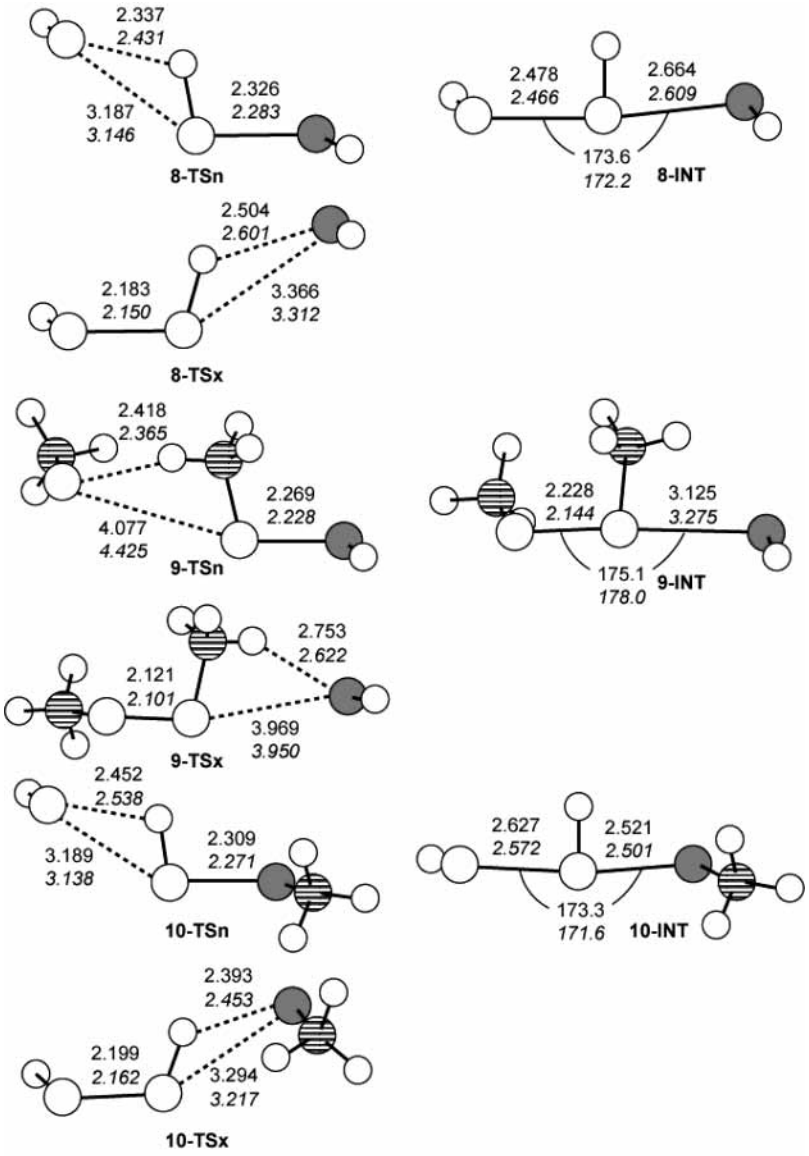

Figure 3. Optimized structures of the intermediates and transition states in reactions 8−10. See Figures 1 and 2 for all details.

surfaces for reaction 1−7 all possess an intermediate with entrance and exit transition states. This is incompatible with the S_N2 mechanism. Rather, the reaction proceeds via two separate, distinct chemical steps. First, the nucleophile adds to selenium, forming a stable intermediate. Then, in the second step, the leaving group exits. This is the addition−elimination pathway.

While the presence of the intermediate precludes the S_N2 mechanism, if the intermediate sits in a shallow well, one might question whether the reaction does not actually behave in an S_N2 fashion, passing through the intermediate without any real lifetime. This shallow well problem does complicate mechanistic analysis for nucleophilic substitution at sulfur where well depths are typically less than 5 kcal mol^{-1}, sometimes even less than 1 kcal mol^{-1}. However, the intermediates for all of the reactions at selenium examined here have entrance and exit barriers of at least 8 kcal mol^{-1}. These constitute intermediates that should be observable.

The preference for attack at selenium over sulfur is evident in the relative energies of the intermediates of reactions 5−7 compared with those of reactions 8−10. The first pair (reactions 5 and 8) compares thiolate attack on selenium or sulfur of HSSeH, and **5-INT** lies 5.29 kcal mol^{-1} below **8-INT** at B3LYP (6.36 kcal mol^{-1} at MP2). Similarly, **7-INT** lies below **10-INT** (by 6.85 or 9.88 kcal mol^{-1} at B3LYP or MP2, respectively), here comparing thiolate attack at selenium or sulfur of $HSSeCH_3$. Last, the methylthiolate attack on CH_3SSeH is compared in reactions 6 and 9; **6-INT** lies below **9-INT** by 3.30 or 2.48 kcal mol^{-1} at B3LYP or MP2, respectively. Selenium can therefore more easily accommodate a third ligand than can sulfur, an idea that can be rationalized by the larger size of the selenium atom, the energetically closer orbitals of selenium, and its ability to participate in four electron-three-center bonding.[37] The larger[28] Se−Cl bond energy in $SeCl_3^-$ over the S−Cl bond in SCl_3 is consistent with the preference of selenium attack described here.

There is also a kinetic preference for attack at selenium over sulfur to form these hypercoordinated intermediates. The relative energy of transition states for reactions of thiolates with simple disulfides range from −8 to −13 kcal mol^{-1},[22] the higher energy for attack at sulfur bearing a methyl group and the lower energy for attack at sulfur bearing a hydrogen. The same trend is true for the entrance TSs for reactions 8−10.

However, attack at selenium, whether by thiolate or selenolate nucleophiles, transpires through TSs that are lower in energy. The relative energy for the TS when selenolate attacks selenium

TABLE 2: Relative Energies (kcal mol^{-1}) for Reactions 1−7

method	reactants	TS	INT	well depth
		Reaction 1 *syn*		
B3LYP/6-31+G*	0.0	−18.86	−27.89	9.03
B3LYP/aug-cc-pVDZ	0.0	−15.00	−23.22	8.22
MP2/6-31+G*	0.0	−17.05	−26.42	9.37
MP2/aug-cc-pVDZ	0.0	−14.94	−23.43	8.49
		Reaction 1 *anti*		
B3LYP/6-31+G*	0.0	−18.79	−28.07	9.28
B3LYP/aug-cc-pVDZ	0.0	−14.94	−23.40	8.46
MP2/6-31+G*	0.0	−17.06	−26.40	9.34
MP2/aug-cc-pVDZ	0.0	−14.93	−23.41	8.48
		Reaction 2 *syn*		
B3LYP/6-31+G*	0.0	−19.57	−27.72	8.15
MP2/6-31+G*	0.0	−19.12	−27.94	8.82
		Reaction 2 *anti*		
B3LYP/6-31+G*	0.0	−19.32	−27.55	8.23
MP2/6-31+G*	0.0	−18.60	−27.52	8.92
		Reaction 3 *syn*		
B3LYP/6-31+G*	0.0	−10.13	−24.23	14.10
MP2/6-31+G*	0.0	−10.88	−23.92	13.04
		Reaction 3 *anti*		
B3LYP/6-31+G*	0.0	−10.13	−24.17	14.04
MP2/6-31+G*	0.0	−10.77	−23.82	13.05
		Reaction 4 *syn*		
B3LYP/6-31+G*	0.0	−10.51	−24.48	13.97
MP2/6-31+G*	0.0	−12.71	−26.84	14.13
		Reaction 4 *anti*		
B3LYP/6-31+G*	0.0	−9.19	−23.75	14.56
MP2/6-31+G*	0.0	−11.45	−25.60	14.15
		Reaction 5		
B3LYP/aug-cc-pVDZ	0.0	−16.42	−24.89	8.47
MP2/aug-cc-pVDZ	0.0	−15.81	−24.54	8.73
		Reaction 6		
B3LYP/aug-cc-pVDZ	0.0	−16.19	−23.75	7.56
MP2/aug-cc-pVDZ	0.0	−17.60	−25.96	8.36
		Reaction 7		
B3LYP/aug-cc-pVDZ	0.0	−9.26	−20.78	11.52
MP2/aug-cc-pVDZ	0.0	−11.44	−22.29	10.85

TABLE 3: Relative Energies (kcal mol^{-1}) for Reactions 8−10

method	reactants	TSn	INT	TSx	product
		Reaction 8			
B3LYP/aug-cc-pVDZ	0.0	−14.38	−19.60	−15.43	−3.05
MP2/aug-cc-pVDZ	0.0	−13.31	−18.17	−14.59	−2.23
		Reaction 9			
B3LYP/aug-cc-pVDZ	0.0	−9.22	−20.45	−19.84	−13.87
MP2/aug-cc-pVDZ	0.0	−11.62	−23.48	−23.27	−14.26
		Reaction 10			
B3LYP/aug-cc-pVDZ	0.0	−11.75	−13.93	−6.96	7.43
MP2/aug-cc-pVDZ	0.0	−11.47	−13.30	−5.69	9.15

TABLE 4: Deprotonation Free Energy (kcal mol^{-1}) for Simple Sulfides and Selenides

	ΔG(expt)	ΔG(MP2/aug-cc-pVDZ)
CH_3SH	350.6[a]	346.2
H_2S	344.4[b]	340.4
CH_3SeH		339.1
H_2Se	335.2[c]	332.7

[a] Ref 39. [b] Ref 40. [c] Ref 41.

bearing a hydrogen (reactions 1 and 2) ranges from −14 to −19 kcal mol^{-1}, depending on the computational method. The TSs are slightly less stable (−9 to −13 kcal mol^{-1}) for attack at selenium bearing a methyl group (reactions 3 and 4). A similar trend holds when the nucleophile is a thiolate: the relative TS energies for reaction 5 and 6, where selenium carries a hydrogen, are lower (about −16 kcal mol^{-1}) than when it carries a methyl group (around −10 kcal mol^{-1} for reaction 10). Therefore, the barrier for attack at selenium is lower than for attack at sulfur.

Comparing gas-phase computational data with results from solution-phase experiments is a dangerous game. Solvent can play an enormous role, especially for reactions involving charged species.[30,38] Nevertheless, our gas-phase computations agree with the limited experimental results for nucleophilic attack at selenium. Both our gas-phase computations and solution-phase experiments suggest a strong kinetic preference for nucleophilic attack at selenium over sulfur. There is no experimental evidence for stable hypercoordinate selenium species in the solution-phase experiments. Hopefully, gas-phase studies will be forthcoming and can test our prediction of stable hypercoordinate organoselenium anions.

Conclusions

Gas-phase nucleophilic substitution at selenium occurs via an addition−elimination mechanism. We have examined seven representative substitution reactions involving different nucleophiles (HS^-, CH_3S^-, HSe^-, and CH_3Se^-) and different substrates (the selenosulfides HSeSH, $HSeSCH_3$, and CH_3SeSH and diselenides HSeSeH, $HSeSeCH_3$, and $CH_3SeSeCH_3$). For all of these reactions, a stable intermediate is located, along with entrance and exit transition states. The intermediates sit in wells of depths of 8 to 14 kcal mol^{-1}, much deeper than the wells for the intermediates for nucleophilic substitution at sulfur.

The S−Se bond, present in a number of selenoproteins, has been implicated in the activity of these proteins. The typical cellular nucleophile is glutathione. We employed thiolates as the nucleophile to model glutathione and simple selenosulfides to model this S−Se protein bridge. In all three cases we examined, attack at selenium is both kinetically and thermodynamically favored over attack at sulfur. Further examination of the reactivity of selenoproteins and development of inhibitors, etc., should concentrate on reaction at the selenium center.

Acknowledgment. The research was supported by the National Science Foundation (CHE-0307260), the Robert A. Welch Foundation (W-1442), and the Petroleum Research Fund, administered by the American Chemical Society.

Supporting Information Available: Coordinates of all optimized structures, their absolute energies, and number of imaginary frequencies. This material is available free of charge via the Internet at http://pubs.acs.org.

References and Notes

(1) Chen, J.; Berry, M. J. *J. Neurochem.* **2003**, *86*, 1−12.
(2) Behne, D.; Kyriakopoulos, A. *Annu. Rev. Nutr.* **2001**, *21*, 453−473.
(3) Arteel, G. E.; Sies, H. *Environ. Toxicol. Pharmacol.* **2001**, *10*, 153−158.
(4) Powis, G.; Montfort, W. R. *Annu. Rev. Pharmacol. Toxicol.* **2001**, *2001*, 261−295.
(5) Mustacich, D.; Powis, G. *Biochem. J.* **2000**, *346*, 1−8.
(6) Schomburg, L.; Schweiser, U.; Holtmann, B.; Flohe, L.; Sendtner, M.; Kohrle, J. *Biochem. J.* **2003**, *270*.
(7) Hill, K. E.; Zhou, J.; McMahan, W. J.; Motley, A. K.; Atkins, J. F.; Gesteland, R. F.; Burk, B. F. *J. Biol. Chem.* **2003**, *278*, 13640−13646.
(8) Klotz, L.-O.; Sies, H. *Toxicol. Lett.* **2003**, *140−141*, 125−132.
(9) St. Germain, D. L. *Trends Endocrinol. Metab.* **1994**, *5*, 36−42.
(10) Zhong, L. W.; Arner, E. S. J.; Holmgren, A. *Proc. Natl. Acad. Sci. U.S.A.* **2000**, *97*, 5854−5859.
(11) Arner, E. S. J.; Holmgren, A. *Eur. J. Biochem.* **2000**, *267*, 6102−6109.

(12) Mugesh, G.; du Mont, W. W.; Wismach, C.; Jones, P. G. *ChemBioChem* **2002**, *3*, 440−447.
(13) Ma, S.; Hill, K. E.; Burk, R. F.; Caprioli, R. M. *Biochem.* **2003**, *42*, 9703−9711.
(14) Kice, J. L.; Slebocka-Tilk, H. *J. Am. Chem. Soc.* **1982**, *104*, 7123−7130.
(15) Rabenstein, D. L.; Scott, T. M.; Guo, W. *J. Org. Chem.* **1991**, *56*, 4176−4181.
(16) (a) Whitesides, G. M.; Lilburn, J. E.; Szajewski, R. P. *J. Org. Chem.* **1977**, *42*, 332. (b) Wilson, J. M.; Bayer, R. J.; Hupe, D. J. *J. Am. Chem. Soc.* **1977**, *99*, 7922−7926. (c) Freter, R.; Pohl, E. R.; Hupe, D. J. *J. Org. Chem.* **1979**, *44*, 1771−1774. (d) Szajewski, R. P.; Whitesides, G. M. *J. Am. Chem. Soc.* **1980**, *102*, 2011. (e) Whitesides, G. M.; Houk, J.; Patterson, M. A. K. *J. Org. Chem.* **1983**, *48*, 112−115. (f) Hupe, D. J.; Pohl, E. R. *Isr. J. Chem.* **1985**, *26*, 395−399. (g) Singh, R.; Whitesides, G. M. *J. Am. Chem. Soc.* **1990**, *112*, 1190−1197. (h) Singh, R.; Whitesides, G. M. *J. Am. Chem. Soc.* **1990**, *112*, 6304−6309. (i) Lees, W. J.; Whitesides, G. M. *J. Org. Chem.* **1993**, *58*, 642−647. (j) Rabenstein, D. L.; Yeo, P. L. *J. Org. Chem.* **1994**, *59*, 4223−4229.
(17) Pleasants, J. C.; Guo, W.; Rabenstein, D. L. *J. Am. Chem. Soc.* **1989**, *111*, 6553−6558.
(18) (a) Engman, L.; Stern, D. *J. Org. Chem.* **1994**, *59*, 5179−5183. (b) Engman, L.; Gupta, V. *J. Org. Chem.* **1997**, *62*, 157−173. (c) Henriksen, L.; Stuhr-Hansen, N. *J. Chem. Soc., Perkin Trans. 1* **1999**, 1915−1916.
(19) Bachrach, S. M.; Mulhearn, D. C. *J. Phys. Chem.* **1996**, *100*, 3535−3540.
(20) Mulhearn, D. C.; Bachrach, S. M. *J. Am. Chem. Soc.* **1996**, *118*, 9415−9421.
(21) Bachrach, S. M.; Gailbreath, B. D. *J. Org. Chem.* **2001**, *66*, 2005−2010.
(22) Bachrach, S. M.; Hayes, J. M.; Dao, T.; Mynar, J. L. *Theor. Chem. Acc.* **2002**, *107*, 266−271.
(23) Bachrach, S. M.; Woody, J. T.; Mulhearn, D. C. *J. Org. Chem.* **2002**, *67*, 8983−8990.
(24) Bachrach, S. M.; Chamberlin, A. C. *J. Org. Chem.* **2003**, *68*, 4743−4737.
(25) Hayes, J. M.; Bachrach, S. M. *J. Phys. Chem. A* **2003**, *107*, 7952−7961.
(26) Gailbreath, B. D.; Pommerening, C. A.; Bachrach, S. M.; Sunderlin, L. S. *J. Phys. Chem. A* **2000**, *104*, 2958−2961.
(27) Bachrach, S. M.; Hayes, J. M.; Check, C. E.; Sunderlin, L. S. *J. Phys. Chem. A* **2001**, *105*, 9595−9597.
(28) Lobring, K. C.; Hao, C.; Forbes, J. K.; Ivanov, M. R. J.; Bachrach, S. M.; Sunderlin, L. S. *J. Phys. Chem. A* **2003**, *107*, 11153−11160.
(29) Aida, M.; Nagata, C. *Chem. Phys. Lett.* **1984**, *112*, 129−132.
(30) (a) Brauman, J. I.; Olmstead, W. N.; Lieder, C. A. *J. Am. Chem. Soc.* **1974**, *96*, 4030−4031. (b) Olmstead, W. N.; Brauman, J. I. *J. Am. Chem. Soc.* **1977**, *99*, 4219−4278. (c) Pellerite, M. J.; Brauman, J. I. *J. Am. Chem. Soc.* **1980**, *102*, 5993−5999. (d) Wilbur, J. L.; Brauman, J. I. *J. Am. Chem. Soc.* **1991**, *113*, 9699−9701.
(31) (a) Hehre, W. J.; Radom, L.; Schleyer, P. v. R.; Pople, J. A. *Ab Initio Molecular Orbital Theory*; John Wiley and Sons: New York, 1986. (b) Cramer, C. J. *Essentials of Computational Chemistry. Theories and Models*; John Wiley: Chichester, UK, 2002.
(32) (a) Becke, A. D. *J. Chem. Phys.* **1993**, *98*, 5648−5650. (b) Lee, C.; Yang, W.; Parr, R. G. *Phys. Rev. B* **1988**, *37*, 785−789. (c) Vosko, S. H.; Wilk, L.; Nusair, M. *Can. J. Phys.* **1980**, *58*, 1200−1211. (d) Stephens, P. J.; Devlin, F. J.; Chabalowski, C. F.; Frisch, M. J. *J. Phys. Chem.* **1994**, *98*, 11623−11627.
(33) (a) Chandrasekhar, J.; Andrade, J. G.; Schleyer, P. v. R. *J. Am. Chem. Soc.* **1981**, *103*, 5609−5612. (b) Saunders, W. H., Jr. *J. Phys. Org. Chem.* **1994**, *7*, 268−271. (c) Merrill, G. N.; Kass, S. R. *J. Phys. Chem.* **1996**, *100*, 17465−17471.
(34) Dunning, T. H. J. *J. Chem. Phys.* **1989**, *90*, 1007−1023.
(35) Frisch, M. J.; Trucks, G. W.; Schlegel, H. B.; Scuseria, G. E.; Robb, M. A.; Cheeseman, J. R.; Zakrzewski, V. G.; Montgomery, J. A. J.; Stratmann, R. E.; Burant, J. C.; Dapprich, S.; Millam, J. M.; Daniels, A. D.; Kudin, K. N.; Strain, M. C.; Farkas, O.; Tomasi, J.; Barone, V.; Cossi, M.; Cammi, R.; Mennucci, B.; Pomelli, C.; Adamo, C.; Clifford, S.; Ochterski, J.; Petersson, G. A.; Ayala, P. Y.; Cui, Q.; Morokuma, K.; Malick, D. K.; Rabuck, A. D.; Raghavachari, K.; Foresman, J. B.; Cioslowski, J.; Ortiz, J. V.; Baboul, A. G.; Stefanov, B. B.; Liu, G.; Liashenko, A.; Piskorz, P.; Komaromi, I.; Gomperts, R.; Martin, R. L.; Fox, D. J.; Keith, T.; Al-Laham, M. A.; Peng, C. Y.; Nanayakkara, A.; Gonzalez, C.; Challacombe, M.; Gill, P. M. W.; Johnson, B.; Chen, W.; Wong, M. W.; Andres, J. L.; Gonzalez, C.; Head-Gordon, M.; Replogle, E. S.; Pople, J. A. Gaussian-98; Gaussian, Inc.: Pittsburgh, PA, 1998.
(36) Frisch, M. J.; Trucks, G. W.; Schlegel, H. B.; Scuseria, G. E.; Robb, M. A.; Cheeseman, J. R.; Montgomery, J. J. A.; Vreven, T.; Kudin, K. N.; Burant, J. C.; Millam, J. M.; Iyengar, S. S.; Tomasi, J.; Barone, V.; Mennucci, B.; Cossi, M.; Scalmani, G.; Rega, N.; Petersson, G. A.; Nakatsuji, H.; Hada, M.; Ehara, M.; Toyota, K.; Fukuda, R.; Hasegawa, J.; Ishida, M.; Nakajima, T.; Honda, Y.; Kitao, O.; Nakai, H.; Klene, M.; Li, X.; nox, J. E.; Hratchian, H. P.; Cross, J. B.; Adamo, C.; Jaramillo, J.; Gomperts, R.; Stratmann, R. E.; Yazyev, O.; Austin, A. J.; Cammi, R.; Pomelli, C.; Ochterski, J. W.; Ayala, P. Y.; Morokuma, K.; Voth, G. A.; Salvador, J.; Dannenberg, J. J.; Zakrzewski, V. G.; Dapprich, S.; Daniels, A. D.; Strain, M. C.; Farkas, O.; Malick, D. K.; Rabuck, A. D.; Raghavachari, K.; Foresman, J. B.; Ortiz, J. V.; Cui, Q.; Baboul, A. G.; Clifford, S.; Cioslowski, J.; Stefanov, B. B.; Liu, G.; Liashenko, A.; Piskorz, P.; Komaromi, I.; Martin, R. L.; Fox, D. J.; Keith, T.; Al-Laham, M. A.; Peng, C. Y.; Nanayakkara, A.; Challacombe, M.; Gill, P. M. W.; Johnson, B.; Chen, W.; Wong, M. W.; Gonzalez, C.; Pople, J. A. Gaussian-03; Gaussian, Inc.: Pittsburgh, PA, 2003.
(37) (a) Hach, R. J.; Rundle, R. E. *J. Am. Chem. Soc.* **1951**, *73*, 4321−4324. (b) Pimentel, G. C. *J. Chem. Phys.* **1951**, *19*, 446−448. (c) Reed, A. E.; Schleyer, P. v. R. *J. Am. Chem. Soc.* **1990**, *112*, 1434−1445. (d) Kaupp, M.; van Wuellen, C.; Franke, R.; Schmitz, F.; Kutzelnigg, W. *J. Am. Chem. Soc.* **1996**, *118*, 11939−11950. (e) Landrum, G. A.; Goldberg, N.; Hoffmann, R. *J. Chem. Soc., Dalton Trans.* **1997**, 3605−3613.
(38) (a) Tanaka, K.; Mackay, G. I.; Payzant, J. D.; Bohme, D. K. *Can. J. Chem.* **1976**, *54*, 1643−1659. (b) Regan, C. K.; Craig, S. L.; Brauman, J. I. *Science* **2002**, *295*, 2245−2247.
(39) Bartmess, J. E.; Scott, J. A.; McIver, R. T. J. *J. Am. Chem. Soc.* **1979**, *101*, 6046−6056.
(40) Rempala, K.; Ervin, K. M. *J. Chem. Phys.* **2000**, *112*, 4579−4590.
(41) Stoneman, R. C.; Larson, D. J. *J. Phys. B* **1986**, *19*, 405−409.